Neutron Reflectivity Investigation of the Propagation of a Melt Polymer across a Glassy Interface

CHRNS School on Methods and Applications of SANS and NR

NIST Center for Neutron Research

October 2022

1 Introduction

The chain-like structure of polymer gives rise to many special effects that are unique to polymer materials science.[1] The universal features dominating the polymer dynamics under thermal and compositional equilibrium, i.e. Rouse motion,[2] entanglement[3] and reputation[4] are all originated from the essential connectivity of polymer chains. The Rouse model[2] is the foundation upon which the most current and more sophisticated interpretations of polymer dynamics are built. The basic assumption in Rouse model is that each individual "bead" (or polymer segment) in the molecule feels the same friction and the macromolecule feels the cumulative effect.[2] However, this mean-field assumption is probably inapplicable in many polymer interdiffusion which by definition refers to diffusion across boundaries, surfaces, interfaces and in gradients. Many practical and useful applications, such as welding, coating, adhesion and friction, are concerned with the interdiffusion between two chemically different pure polymers.[5] In these cases, polymers move in an uneven field of thermodynamic interactions, and the friction experienced by each individual

bead depends on the its neighboring environment as the interdiffusion process is proceeding. A schematic of interdiffusion between two different polymers is shown in Figure 1.

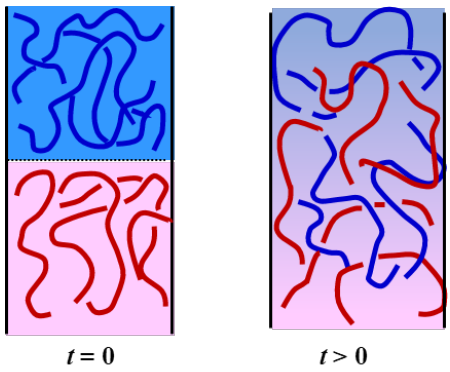

Figure 1 Schematic of interdiffusion at polymer interface

When one polymer is placed into contact with another polymer, the nascent interfacial region is limited to monomeric segment, a question naturally arises about what the forces are that shape the interface between the two different phases. First, it is necessary that the components, at least one component, have certain mobility (which may be achieved by controlling temperature) so that further physical interpenetration can proceed. Second, two components should be thermodynamically compatible to a certain extend. The first response of the interfacial segments (which may be spatially away from the center of mass of the large polymer coil) to the chemical potential gradient will initialize the intermixing (penetration, adsorption) process. Last, if the polymer pair is with mismatch in their respective molecular mobilities, such as the case that one of the components is a glassy solid and the other is in melt state, due to the viscoelastic nature of the polymer, the initial relaxation of the interfacial segments will introduce a series of relaxation and generate a supplementary stress gradient which in turn will modify the transport process itself. An example of the prominent diffusion-relaxation feedback mechanism is a diluent propagates into a glassy polymer by the so-called case-II diffusion,[6] where the rate of penetration of the diluent

is governed by the deformation resistance of the solid polymer that was considered to be its viscosity-albeit modified by the plasticization effect of the sorbed diluent.[7] Overall, in a common interdiffusion process, the description of interfacial evolution brings thermodynamics and polymer relaxation into role, and it requires fundamental understanding of how specific molecules interact and response under the complex feedback mechanism.

In this work, we examine the interfacial evolution between two different polymers, i.e. deuterated polycarbonate (*d*PC) and hydrogenated poly (methyl methacrylate) (*h*PMMA). Unlike the Fickian diffusion of an isotope of an elemental solid into the corresponding pure substance, which is accompanied by negligible material misfit, here, the penetration of a diluent macromolecule (*h*PMMA) into a glassy polymer (*d*PC) is accompanied by a very substantial material misfit. With the penetration of the fast-moving PMMA into the sluggish dPC layer, a visco-plastics extrusion process will be revealed from the analysis of interfacial profiles.

2 Objectives

The objectives of this tutorial experiment are:

a) To learn reflectivity measurements on bilayer polymer thin films.

b) To determine the time evolution of interfacial profile.

c) To play with the chain-like feature of polymers and understand the interplay of thermodynamic effect and kinetic effect on interdiffusion at polymer interfaces.

3 Experiment

3.1 Materials

The molecular mass and the polydispersity of *d*PC used in this study is $M_n = 8.4\times10^4$ g/mol and M_w/M_n = 2.45, respectively. Here, M_n and M_w denote number averaged and weight averaged molecular mass. The theoretical calculated values of the radius of gyration (R_g) for this *d*PC is 11.0 nm.[8] The T_g of *d*PC is ~ 145 °C. The molecular mass and the polydispersity of PMMA used in this study is $M_n = 5.0\times10^4$ g/mol and $M_w/M_n = 1.10$, respectively. The theoretical calculated values of R_g for this PMMA is 5.7 nm.[8] The T_g of PMMA is ~ 115 °C. It should be noted that, the average molecular weight between entanglement points (M_e) for PC is 1,660, which is equivalent to 6.5 repeating units and is abnormally small as compared to that of PMMA (M_e = 12,500).[8]

3.2 Bilayer film preparation

The samples prepared for the NR experiment were *d*PC/PMMA bilayer films consisted of a dPC layer on top of a PMMA layer with polished silicon wafers as substrates (7.5 cm diameter, 0.5 cm thickness). The schematic of the bilayer film is shown in Figure 2. The bilayer samples were prepared by spin-coating and floating techniques. Prior to spin coating, the silicon wafers were cleaned by a treatment with freshly prepared "piranha" solution (70/30 v/v H_2SO_4 (50%)/ H_2O_2 (30%)) at 90-100 °C for 45 minutes and then rinsed with copious amount of distilled water and dried with a stream of technical grade nitrogen. Next, the silicon oxide layer was removed from the cleaned wafer by etching in a 5% HF solution. Approximately 35 nm thick PMMA layer was deposited on the wafer from the PMMA solution prepared in toluene by spin coating at 2500 rpm. The cast PMMA layer was annealed at 130 °C for 2 h under vacuum to remove any residual solvent and relax the stresses built during the spin coating process. The top *d*PC layer (approximately 70 nm thick) was prepared by spin coating a solution of dPC in 1, 1, 2, 2- tetrachloroethane on another clean silicon wafer. By immersing the wafer into distilled water, the *d*PC layer was floated off onto the water surface and then picked up on the wafer which has been spin-coated with PMMA in

advance. Bilayer films were placed under vacuum at 90 ºC for 24 h to remove residual solvent and water trapped between the layers before use. X-ray reflectivity (Bruker, D8-Ddvance) was used to characterize the single films with respect to film thickness and surface roughness.

Figure 2. Schematic of the bilayer samples. When the sample is annealed at 130 - 145 ºC, the *d*PC is in the sluggish glass transition state and the *h*PMMA is in the liquidly melt state.

3.3 Interdiffusion

Interdiffusion was accomplished by inserting the bilayer sample in a large slotted aluminum block, preheated to desired temperatures in vacuum oven. The temperature was controlled to ± 0.2 ºC. After a desired interdiffusion time, the specimens were removed from the vacuum oven and quenched to room temperature by placing the substrate on a cool metal block, which will halt the interdiffusion process. All reflectivity experiments were performed at room temperature.

3.4 NG7 Horizontal Neutron Reflectometer

Reflectivity measurements were performed on the NG7 horizontal reflectometer. The schematic of NG7 reflectometry is shown in Figure 3. The wavelength (λ) of the neutron used is 0.475 nm with $\Delta\lambda/\lambda \approx 0.02$. A tilting pyrolytic graphite monochromator is located at the bottom 1 cm of guide NG7. The resulting beam profile is approximately 50 mm in width with a maximum height of 10 mm. The beam is filtered against thermal neutrons after the monochromator with a liquid nitrogen cooled beryllium filter. The neutron flight tubes have $2\theta_c$ super mirrors mounted on their vertical surfaces to reduce losses due to horizontal beam divergence. All flight tubes have single crystal

sapphire windows and are evacuated to reduce losses from air scattering. The pre- and post-sample flight paths are 2 m in length, and each has a pair of independently controlled LiF slits for collimation of the incident or scattered beam. Horizontal collimation is also available before and after the sample position. A beam monitor detector located after the second collimating slit samples a portion of the beam incident on the sample and allows the primary detector data to be scaled to absolute reflectivity. The instrument has two available detectors: (1) a 2.5 cm diameter cylindrical 3He proportional counter or (2) an ORDELA linear position sensitive 3He proportional counter with a 10 cm position-sensitive length and a 4 cm width. The detector is used without the final set of collimation slits.

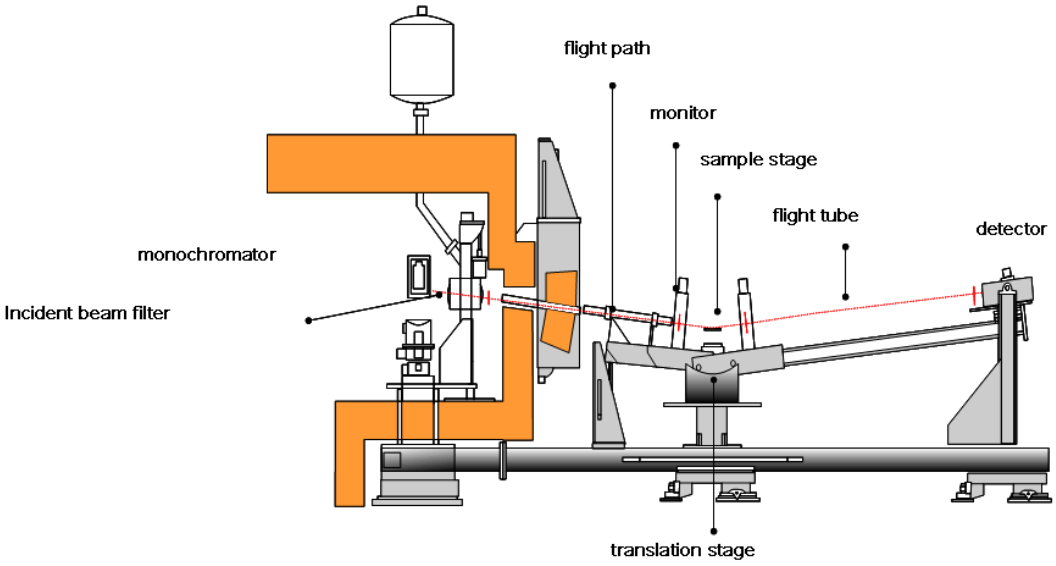

Figure 3. Schematic of NG7 horizontal neutron reflectometer.

3.5 Data collection and data reduction

The reflectivity measurements were performed over a range of angles and the data was presented as a function of the neutron momentum transfer perpendicular to the surface, $q = (4\pi/\lambda)\sin\theta$, where θ is the incident angle of the neutron radiation. The angular divergence of the beam was varied

through the reflectivity scan and this provided a relative q resolution $\Delta q / q$ of 0.04. The neutron reflectivity is calculated from the measured specular raw data, the background data and the incident beam data. This process is called data reduction. Data reduction uses the NCNR online software 'Reductus'.[9] To calculate the neutron reflectivity, the background intensity is subtracted from the specular reflectivity and the difference is divided by the incident beam intensity, as shown by the module in Figure 4. This obtained ratio, the neutron reflectivity, is always ≤ 1 (not shown).

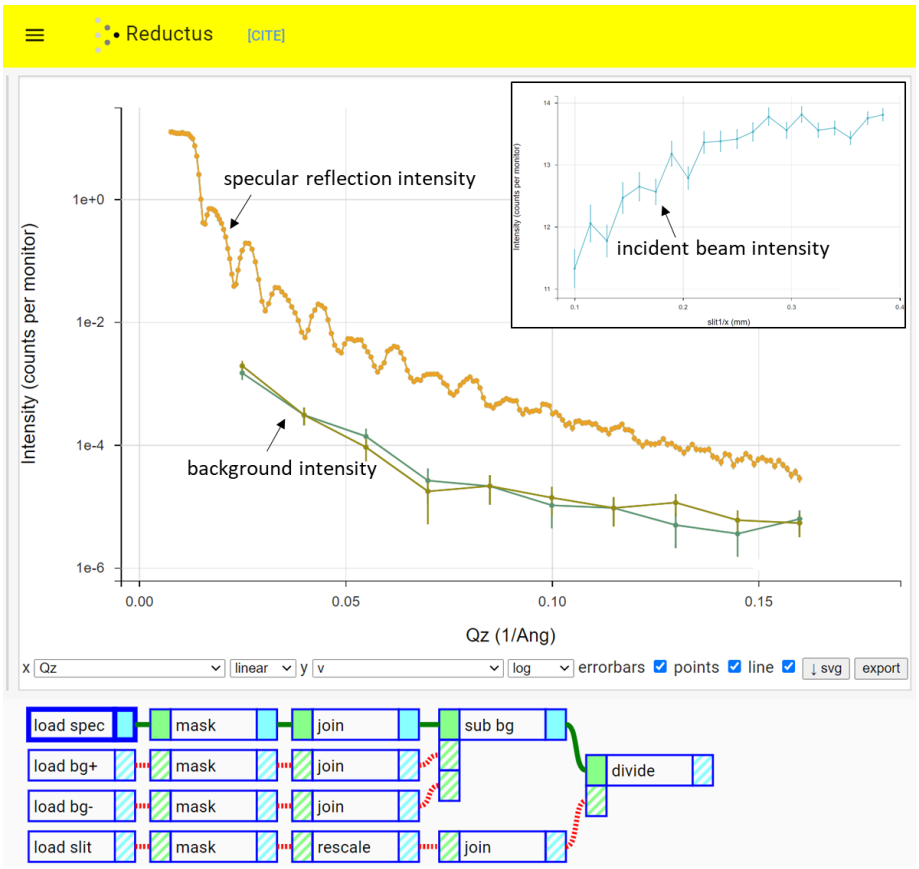

Figure 4. Data reduction using the NCNR online software 'Reductus' (https://reductus.nist.gov).

4. Data analysis

Reflectivity observations are sensitive to the in-plane averaged neutron scattering length density (*SLD)* profile perpendicular to the sample surface. The *SLD* values for *d*PC, PMMA and bulk

silicon are 3.28×10^{-4}, 1.06×10^{-4} and 2.07×10^{-4} nm^{-2}, respectively. The change in the NR curve as a function of annealing time is demonstrated in Figure 5, with each respective spectrum offset log $R = 1$ for clarity. Apparently, the reflectivity curve changes as intermixing keeps going. NR data was fit using Refl1D program.[9] In this program a model *SLD* profile is proposed as a layered structure of material "slabs". Each slab is described by three parameters: *SLD*, thickness, and width of the interface with the next layer. The corresponding evolution of *SLD* profiles are also presented in Figure 5.

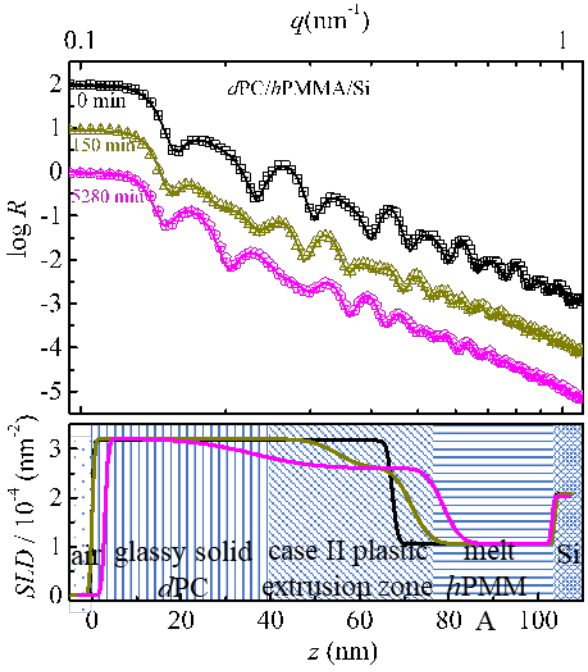

Figure 5. Neutron reflectivity spectra (up) and the corresponding evolution of *SLD* profile (down) for a *d*PC/*h*PMMA/Si bilayer sample as made (0 min) and after annealing at 145 ºC for 150 min and 5280 min. The symbols are the experimental data and the solid lines are the theoretical fits to the data from model density profiles.

In general, error functions are used to fit interfacial profiles, including those between air/*d*PC and *h*PMMA/silicon interface. The profile for the as-made sample can be successfully fitted by

assuming a diffuse Gaussian roughness at the *d*PC/*h*PMMA interface. But when the fast moving PMMA molecules enter the glassy *d*PC matrix, asymmetric concentration profiles are captured. A snapshot of penetration profile can be characterized by three zones, glassy solid, melt and a diluent-laden zone in between. Furthermore, the diluent-loaded zone can be separated into two phases, a partly-relaxed precursor front which presents a smooth concentration gradient and a fully-relaxed rubbery phase in which the concentration gradient is negligible. The evolution of the interfacial profiles reveals a plastic-extrusion process.

References

(1) Kausch, H. H.; Tirrell, M. *Annu. Rev. Mater. Sci.* **1989,** *19*, 341.

(2) Rouse, P. E. *J. Chem. Phys.* **1953,** *21*, 1272.

(3) Edwards, S. F. *Proc. Phys. Soc.* **1967,** *92*, 9.

(4) de Gennes, P. G., *Scaling Concepts in Polymer Physics*. Cornell University Press, Ithaca, New York, 1979.

(5) Yuan, B. L.; Wool, R. P. *Polym. Eng. Sci.* **1990,** *30*, 1454.

(6) Alfrey, T.; Gurnee, E. F.; Lloyd, W. G. *J Polymer Sci* **1966**, 12, 249.

(7) Thomas, N. L.; Windle, A. H. *Polymer* **1982**, *23*, 529.

(8) Fetters, L. J.; Lohse, D. J.; Colby, R. H., ‘‘Chain dimensions and entanglement spacings,’’ in Physical Properties of Polymers Handbook, edited by Mark, J. E.. AIP, New York, 1996.

(9) Kienzle, P. A.; Maranville, B. B.; O'Donovan, K. V.; Ankner, J. F.; Berk, N. F. and Majkrzak C. F. https://www.nist.gov/ncnr/reflectometry-software 2017-